GELATION OF LOW MOLECULAR WEIGHT MOLECULES WITH POLYMERS FOR SIGNAL AMPLIFICATION IN SENSING

Tracy H. Lent

Undergraduate Honors Thesis

Prepared for:

Professor Anne J. McNeil

5 May 2009

TABLE OF CONTENTS

ACKNOWLEDGMENTS

The past few years doing research has been a huge learning experience. Many of the lessons I have learned have spilled over into other areas of my life, and for that I am grateful. I would like to thank Anne McNeil for all of her guidance, honesty, and support that, overall, has cultivated my creativity and curiosity in my study of the natural world in ways that can not be measured. I would also like to acknowledge the support of many of my fellow lab members, past and present: Erica Lanni, Jonas Locke, Jing Chen, Cheryl Moy, Raja Kaliappan, Yash Adhia, Ming Fang, Mari Brunner, Lydia Benitez, and more. The collaboration has been invaluable: from day to day work in the lab to presentations to cultivating chemistry common sense. Additionally, without the support of family and friends, I probably would have lost my sanity long ago. Last, but most importantly, I want to thank God not only for creating such a complex, intricate, and beautiful world, but for giving all of us the ability to see a tiny glimpse of the enigma that the natural world is. His power and creativity will never cease to amaze me.

ABSTRACT

The need for rapid, reliable sensors has never been greater. The development of sensing techniques has attracted much scientific attention because of their importance in biomedical applications and national security.[1] However, sensors are often constrained by sensitivity and selectivity of detection, in addition to the limitations of sample preparation and the cost of the detector itself. Sensing via analyte-triggered gelation offers a quick, portable alternative to traditional sensors.

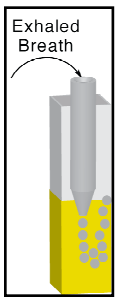

Figure 1: Schematic of proposed sensor.

Our overall goal is to develop a gel-based sensor for breath analysis (Figure 1). Specifically, we are interested in the detection of nitric oxide (NO). Elevated concentrations of NO in the body can indicate a variety of diseases, such as tuberculosis and lung cancer.[2] Current methods of detection involve extensive sample preparation and expensive instrumentation.[3]

We have designed an innovative system utilizing analyte-triggered gelation to detect NO via oxidation-induced planarization of **1** (Dihydropyridine, DHP) to **2** (Pyridine, PYR) (Figure 2).[5] Our current system has a sensitivity of 0.1 parts per thousand, but we need to increase the sensitivity to the parts per billion (ppb) range to be of use in biomedical applications. To address this problem, the specific aims of my project are to improve the sensitivity of this sensor by: (1) Inventing a method of signal amplification utilizing polymers. (2) Determining how signal amplification works. (3) Applying this method to other analyte-triggered gel sensors.

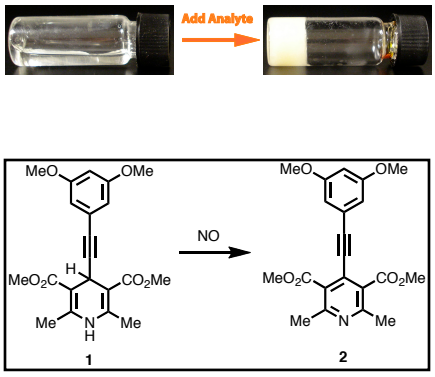

Figure 2: Analyte-triggered gelation upon NO-induced oxidation of **1**.

BACKGROUND

I. MOLECULAR GELS

The discovery and design of small molecules capable of forming gels is a rapidly expanding field.[4] For example, applications utilizing gels include biosensing,[5,6] regenerative medicine,[7] and smart materials.[8] Though molecular gels have been studied for over 160 years, but the mechanism for gel formation is still largely unknown. Gels are often made by supersaturating a solution via heating and allowing the solution to cool, and gelation is believed to occur when molecules self-assemble and phase-separate to form fibers or other low-dimensional structures. These supramolecular structures become entangled and produce random 3-dimensional network. Solvent molecules become trapped in the fibrous network through surface tension. A stable gel (a soft material that can self support itself upon inversion) is formed if the concentration of gelators exceeds the minimum threshold necessary to form a gel (known as the critical gelation concentration, cgc) (Figure 3). This self-assembly of the small molecules is guided by non-covalent interactions, such as H-bonding, van der Waals interactions, donor-acceptor interactions, and π-stacking. Molecular assembly is recognized as an important component, but the forces that determine whether a crystal or gel forms are still unknown and can be difficult to quantify.

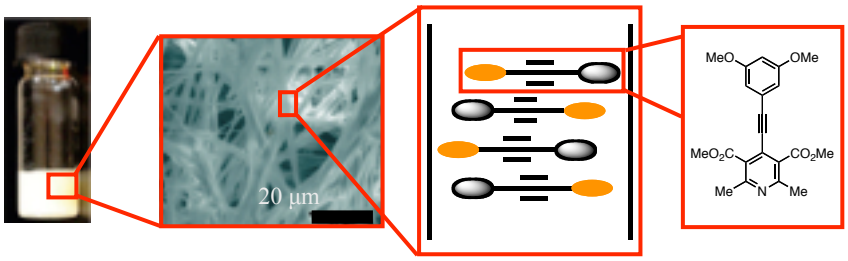

Figure 3: Morphology of a molecular gel.

The nucleation model is the predominant theory in the literature that describes self-assembly as a highly cooperative process. Nucleation is initiated by a high-energy aggregation of small molecules via intermolecular forces. Additionally, solvent molecules play an important role in controlling the self-assembly process from small molecules to bundles and fibers.[9] The formation of nuclei is a dynamic process dominated by the competition between the reduced bulk free energy and the increased surface free energy. The nucleation barrier is dependent upon the structure of the nuclei as well as the degree of supersaturation. Small molecules aggregate and form fibers, and the fibers entangle into bundles that form

a dense, cross-linked network to make up the self-supporting gel. However, the kinetics of this transition has thus far been unclear.[10]

The other model of gel formation is known as crystallographic mismatch branching (CMB). Liu et al.[11] propose that the formation of fibers is controlled by kinetics associated with the nucleation-growth process (Figure 4). Primary fibers are formed by a nucleation process, but the build up of the gel network is controlled by the number of nucleation points. To minimize the energy of interactions, the next small molecules will interact with the growing gel fiber, resulting in a structure whose new layers match with that of the existing surface of the fibers. For any crystallization system, there is a probability for mismatching on the growing gel fiber, and the number of defects is dependent upon both the structural match between the growing gel fiber and and small molecule gelator as well as the degree of supersaturation of the solution. Thus the gel network is formed via a series of nucleation sites, fiber growth, and crystallographic mismatch sites that give new nucleation sites.

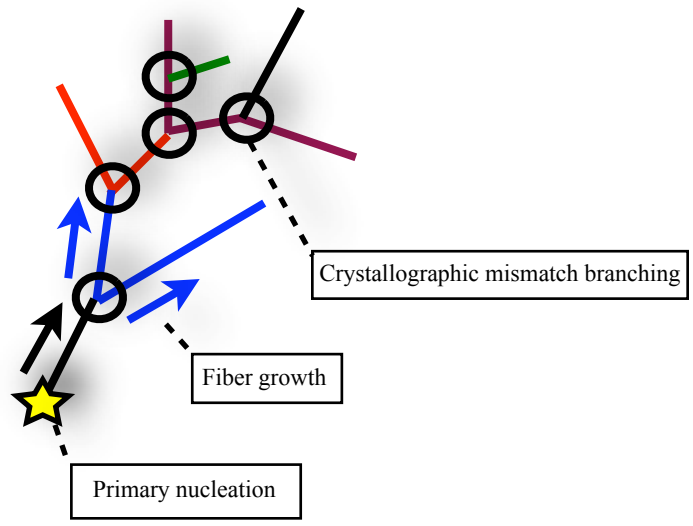

Figure 4: Schematic of crystallographic mismatch branching (CMB).

To summarize, the two approaches give two different perspectives on the self-assembly of low molecular weight gelators: the former focuses on the molecular aggregation, and physical cross-links of the fibers give rise to the self-supporting material. The latter takes a macroscopic perspective, where the emphasis is on the branching of fiber junctions to build up the gel.

II. RESPONSIVE GELS

Sensors are important to detect a variety of analytes, and detection has traditionally been achieved in a number of ways, such as polymer adsorption (mass detection),[12] displacement immunoassays,[12] fluorescence quenching,[13] and other forms of optical modulation.[14]

Gels have emerged in the literature relatively recently as sensors and are quickly emerging as promising alternatives to traditional sensors. The design of a stimuli-induced gelator is very difficult because of the need to design a precursor molecule that does not form a gel. Xu et al.[6] have developed a stimuli-induced gelation system to detect inhibitors of the enzyme β-lactamase by appending a solubilizing group to a known gelator.[15] A hydrophilic group was appended to a known gelator that prevented gel formation. When the enzyme was active (no inhibitor), the linkage between the gelator and hydrophilic group was cleaved to allow the gelators to self assemble into a gel (Figure 5). While successful, this approach has been limited to few triggers. Another strategy is to promote self-assembly by triggering changes in the intermolecular or molecule-molecule interactions, such as light-induced isomerizations[16] or employing additives[17] to influence molecular packing. While it is difficult to predict whether the molecular change will more strongly effect the solubility or intermolecular interactions, we believe that this approach is more promising for designing new triggered gelations.

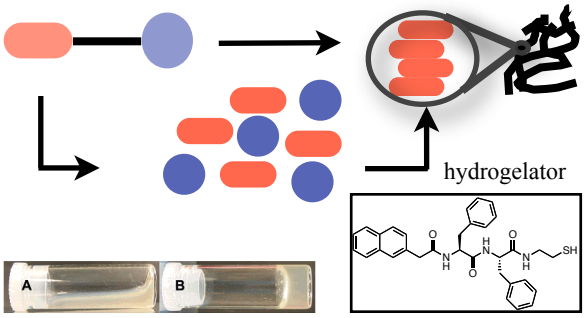

Figure 5: An example of stimuli-induced gelation.[6]

We have designed an analyte-triggered gelation based on this second approach. In the presence of analyte, **1** is oxidized and the molecule goes from its bent conformation to linear **2** (Figures 6, 7). This system can form a gel in the

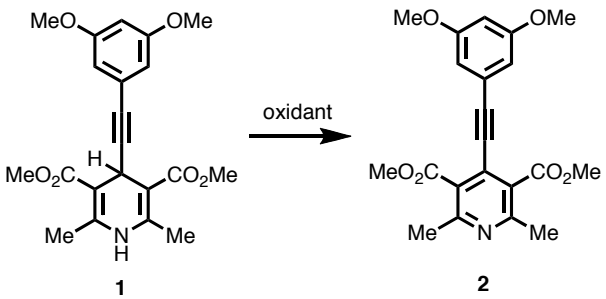

Figure 6: Oxidation of **1** (DHP) gives **2** (PYR), a gelator.

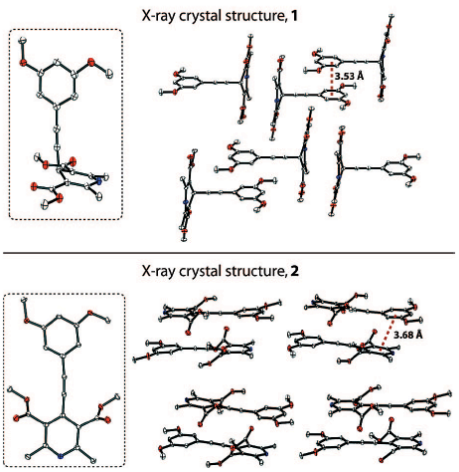

Figure 7: X-ray crystal structures of **1** (top) and **2** (bottom).

presence of a strong oxidant, ceric ammonium nitrate (CAN), in a variety of different organic/water mixtures.

Nitric oxide (NO) is a biomarker for diseases such as lung cancer and tuberculosis. Gas phase chemiluminescence detection of NO was developed for environmental monitoring in 1970 (Equation 1).[3] Other methods include fluorometric techniques and electrochemical methods, but these methods require extensive sample preparation and expensive instrumentation for analysis. We successfully employed our analyte-triggered gelation system to detect NO in the parts per thousand range. However, this system needs to detect NO in the ppb range to be used in biomedical applications.

$$NO + O_3 \longrightarrow NO_2^* + O_2$$

$$NO_2^* \longrightarrow NO_2 + \text{light}$$

Equation 1: Reaction of NO with O_3 gives excited NO_2^*. As NO_2^* relaxes to the ground state, a photon is released.

III. Two-component Gels

Many two-component gels rely on the initial interaction of distinct individual components to form a complex that subsequently self-assembles into a fibrous gel network. There are two classes of two-component gels. An individual component can be present in solution and only upon addition of the second component will a gel form, or the addition of the second component can significantly modify the behavior of a known gelator (Figure 8).[17] This change in molecular behavior is often due to H-bonding, electrostatics, or donor-acceptor interactions. For instance, **3** forms a gel only in the presence of Ag^+. The metal coordinates **3** into a highly organized supramolecular assembly that allows **3** to H-bond with other molecules of **3**.(Figure 9).[18]

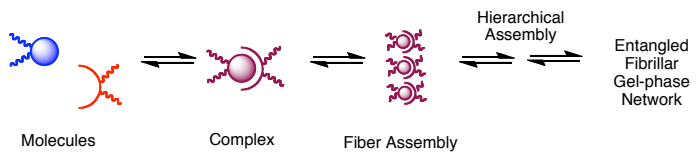

Figure 8: Schematic of the formation of a two-component gel. Only upon formation of a two-component complex will fiber assembly proceed.

One exciting aspect of two-component gels is that there is an

additional element of tunability and control in the self-assembly process that is not seen in one-component gels. For instance, the ratio of two components offers another parameter that can be varied to generate new morphologies and tune the material's behavior (e.g., cgc, molecular recognition, etc.).[11, 19, 20]

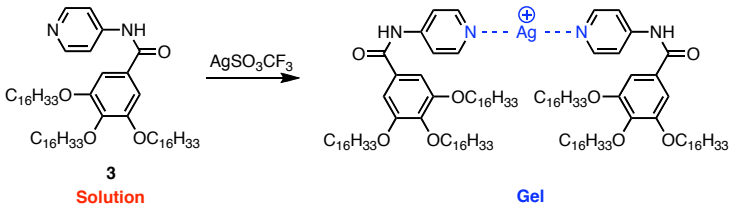

Figure 9: Only upon the addition of $AgSO_3CF_3$ a can a gel of **3** form.

Inspired by the versatility of two-component gel networks, we are currently developing a new method of signal amplification by adding an external crosslinker to decrease the cgc (Figure 10). We also plan to study how the external cross-linker changes the composition of the gel.[21]

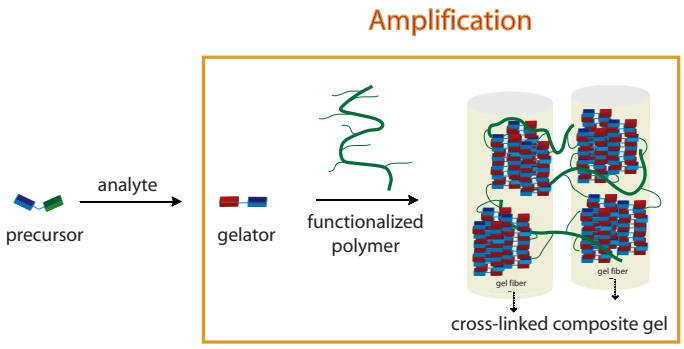

Figure 10: Proposed method of signal amplification with polymers.

PROJECT DESIGN

Stimuli-responsive gelations, like the oxidation-induced gelation shown above, typically use one analyte molecule to form one molecule of gelator; currently, the molecular gels detect a part per thousand concentration range, but to make this a practical sensor, the analytes need to be detected in the parts per billion range.

We propose two approaches to improve a known gelation system by introducing polymers to act as physical cross linkers to decrease the concentration of analyte necessary to form a stable gel (Figure 11). Approach 1 utilizes commercially available functionalized polymers to act as a non-covalent cross-linker. In approach 2, gelator is appended to the polymer backbone.

The long term goals of this project include studies designed to characterize the nature of the interaction between the polymer and gelator. Common methods used in this area include NMR spectroscopy,[22] FT-IR spectroscopy, [23] UV-vis spectroscopy,[24] and powder X-ray diffraction.[25] Additionally, we plan to study the kinetics of the gelation process, the structure of polymers and how it matches to gelator structure and solvent, the effect of polymer on gel strength and structure, and the effect of polymer length and distance between functional groups.

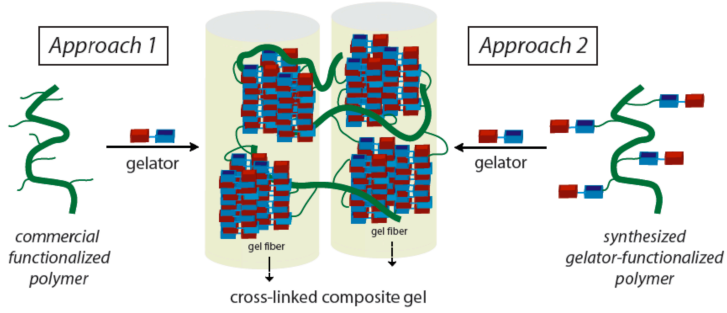

Figure 11: Approach 1 (left) utilizes commercially available polymers for cgc reduction, while approach 2 (right) utilizes synthesized gelator-functionalized polymers.

Approach 1

Since there are a myriad of polymers commercially available, we will focus on polymers with reported solubilites in water/organic solvent mixtures.[26] Preliminary results are promising; upon the addition of poly(acrylic acid) (PAA, ~450 kDa), the critical gelation concentration of **2** was substantially reduced. Moreover, we found that adding polymers facilitates gelation in solvent systems previously unsuitable for gelation. We hypothesize that the reduction of the cgc is due to interactions between the polymer and gelator (e.g., H-bonding, protonation, etc.). We will describe the nature of the interactions between the polymer and gelator using a combination of spectroscopic and microscopic techniques under different gelation conditions. Liu et al. saw a similar effect, which they attributed to the polymer adsorbed to the growing fiber that promoted the mismatch junctions.[11] Future work will include studies distinguishing between the crystallographic mismatch approach and our proposed mechanism involving polymer-gelator interactions.

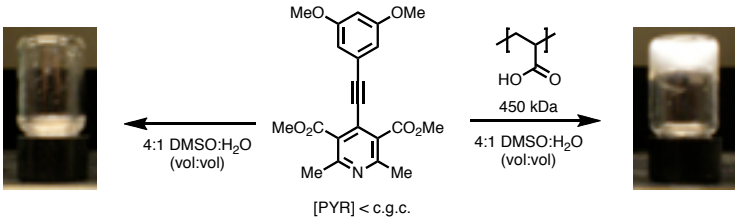

Figure 12: Below the cgc, **2** is not able to form a gel (left). In the presence of PAA (450 kDa), **2** is able to form a stable gel below its cgc (right).

Approach 2

Another approach is to synthesize a series of random copolymers with gelators attached via a linker to the polymer backbone (Scheme 1).[27] A series of screens will help us select ideal polymer backbones and lengths. Some parameters we will look at include: polymer backbone, number of functionalized monomers per copolymer, copolymer length, linker location, and linker length.

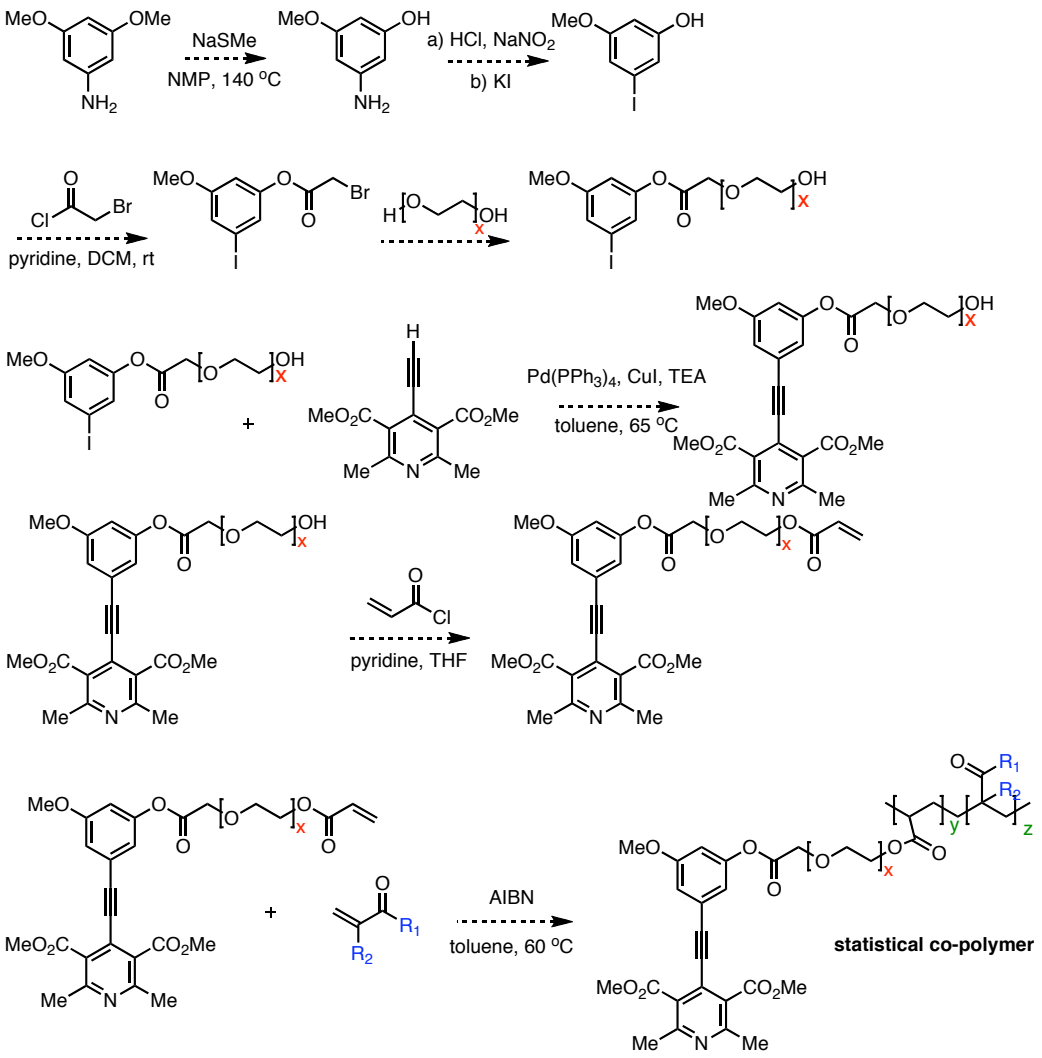

Scheme 1: Proposed synthesis of gelator-appended statistical copolymer.

RESULTS AND DISCUSSION

I. PROOF OF PRINCIPLE

A variety of commercially available polymers were screened for solubility in 4:1 DMSO:H_2O, but only poly(acrylic acid) (PAA), poly(acrylamide), cellulose acetate, hydroxypropyl cellulose, and poly(styrene sulfonate) sodium salt were soluble in this system. None of these polymers formed a gel on their own. Utilizing the heat-cool method, **2** formed a gel below the cgc only in the presence of PAA (Table 1).

Polymer	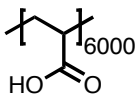	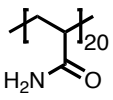	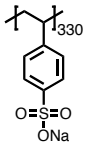	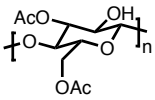	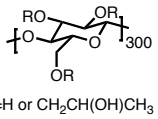
4:1 DMSO:H_2O t > 12 h	Stable gel	No gel formation	Unstable gel	No gel formation	No gel formation

Table 1: Testing the ability of **2** to gel in the presence of commercially available polymers.

The subsequent studies focus on studying the effects of PAA on gelation as this system appeared to be most promising.

The addition of PAA (~450 kDa) to **2** decreased the cgc from 8.5 mg/mL to approximately 6 mg/mL. However, increasing the concentration of PAA did not further reduce the cgc (Figure 13).

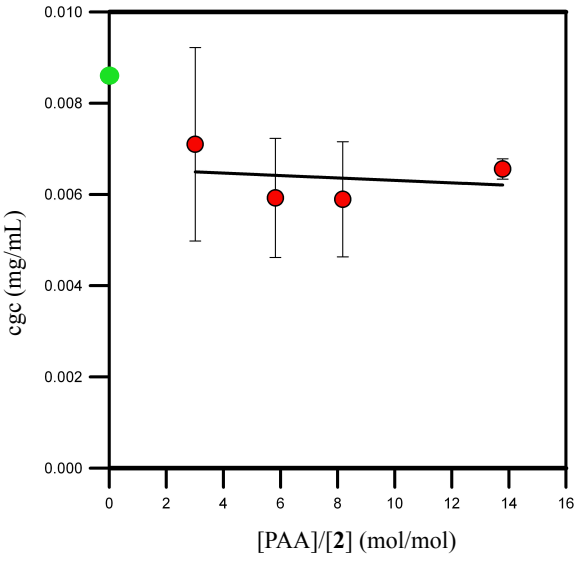

Figure 13: Cgc optimization in 4:1 DMSO:H_2O.

First, we wanted to see what effects changing the functional groups off of the polymer backbone would have on the ability of **2** to form a stable gel below its cgc (Figure 14). However, the derivative P_1 was not soluble in the DMSO:H_2O system. Intriguingly, **2** is not able to form a gel

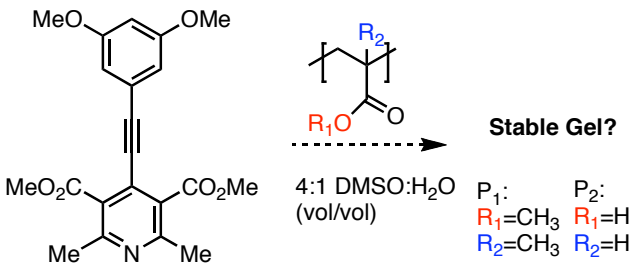

Figure 14: Testing the ability of **2** to gel in the presence of PAA derivatives.

below its cgc in the presence of PAA (450 kDa) with ceric ammonium nitrate (CAN). CAN chelates with the carboxylate groups of PAA; this suggests that the carboxylate groups of PAA play an integral role in the reduction of the cgc of **2**.

Also, we began to study the molecular weight (M_w) dependence of PAA on gelation with **2** (Table 2). It appears that there is a dependence on the ability of **2** to gel in the presence of PAA. More studies are necessary to determine the minimum M_w of PAA necessary to form a gel with **2**, as well as why this dependence exists.

2 (mg)	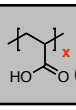 **(0.3 M)**	**Result**
6	x= 1	solution
6	x= 2	fibers formed, no gel
6	x= 3	fibers formed, no gel
6	--	unstable gel
6	x= 6000	stable gel

Table 2: Molecular weight dependence of PAA on gelation.

We also investigated other potential methods to reduce the cgc of **2** (Table S1 in Supporting Information). Overall, the use of polymers to reduce the cgc of a known gelator appears to be more promising than alternate routes.

II. How does PAA effect gel morphology and molecular packing?

In conjunction with studies elucidating potential polymer-gelator interactions, we also wanted to determine if the **2**-PAA gel morphology differed from that of the gel of **2**. Powder X-ray diffraction, polarized Raman scattering, and optical microscope studies indicate that the gel morphologies are similar.

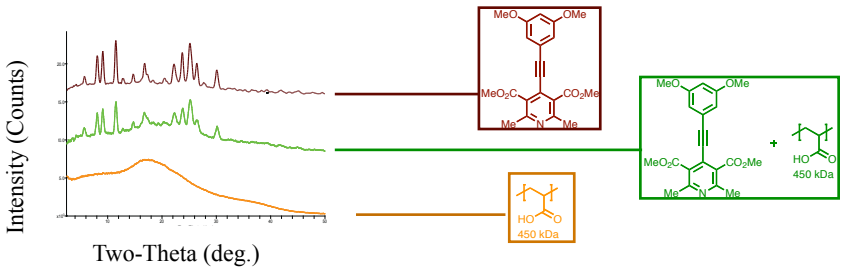

Figure 14: Powder X-ray diffraction.

Powder X-ray diffraction of cryo-dried gel samples indicate that the two gels have similar morphologies (Figure 14).

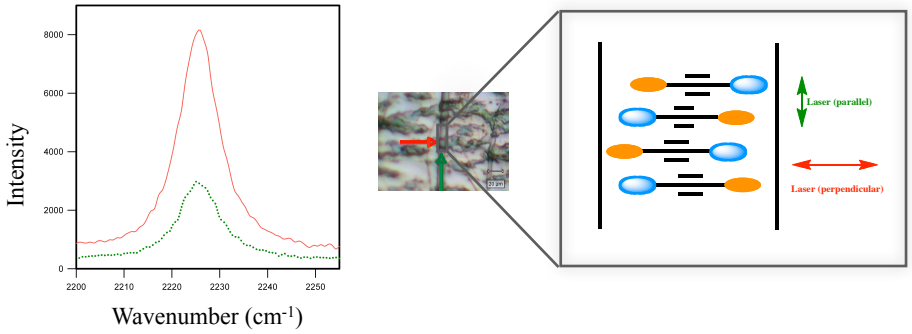

Figure 15: Raman scattering of gel fiber.

Polarized Raman scattering was used to determine the orientation of **2** in the gel fibers. A laser was used to excite **2** in the gel fibers both parallel and perpendicular to the fiber axis. We monitored the scattering of the excitation of the acetylene bond in **2**. The intensity of the acetylene excitation peak was greater when the gel fiber was excited perpendicular to the fiber axis; the increase in intensity indicates that **2** assembles perpendicular to the direction of fiber axis (Figure 15).

Optical microscope comparisons of gels formed with and without PAA give similar hair-like fibers (Figure 16).

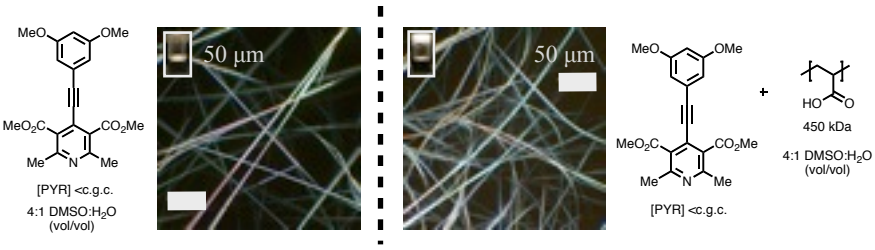

Figure 16: Optical microscope comparison.

Crystals of **2** were grown in 4:1 DMSO:H_2O both with and without 450 kDa PAA.[28] Crystal structures indicate that the molecular packing is also the same whether or not the crystals were obtained in the presence of PAA (Figure 17).

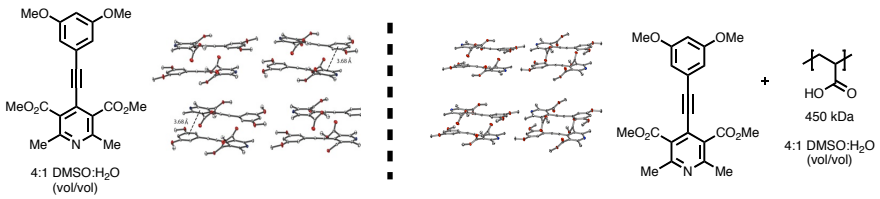

Figure 17: X-ray crystal structure comparison.

III. Is the decreased cgc a pH effect?

We wanted to see if the reduction of cgc in the presence of PAA was due to a decrease in pH.[15] Keeping the pH constant, we compared the ability of **2** to gel (below its cgc) in the presence of 450 kDa PAA and acrylic acid (the monomer unit of PAA). **2** formed a stable gel in the presence of PAA, but in the presence of acrylic acid, a precipitate formed (Figure 18).

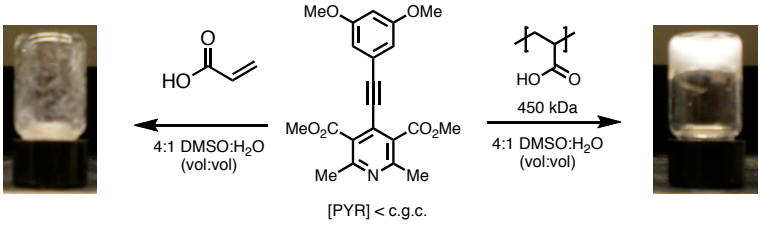

Acid	pH (95% confidence interval)
0.3 M PAA (450 kDa)	4.82-5.41
0.3 M acrylic acid	4.06-5.86

Figure 18: Gelation of **2** in the presence of acrylic acid (left) and 450 kDa PAA (right).

We also tested gelation in the presence of a stronger acid, HCl. Once again, the addition of HCl does not decrease the cgc of **2**, as was seen with acrylic acid (Table 3). Overall, it appears that the polymer is important in the reduction of the cgc and it is not simply a pH effect.

Trial	2 (mg)	Acid	[Acid] (M)	Solvent	Result
A	6	PAA (450 kDa)	2.7×10^{-3}	1.6:1 DMSO:H_2O	Stable Gel
B	6	HCl	2.7×10^{-3}	1.6:1 DMSO:H_2O	Unstable Gel
C	6	none	--	1.6:1 DMSO:H_2O	Stable Gel

Table 3: Gelation of **2** in the presence of different acids.

IV. Is the polymer protonating **2**?

Since the decrease in cgc is not simply a pH effect, we hypothesized that there could be interactions between PAA and **2** that lead to a reduction in cgc (Figure 19). We first hypothesized that there could be protonation of **2** by the carboxylate group of PAA (Figure 20). Literature precent shows that upon protonation of pyridine moieties, a shift in the λ_{max} in the UV-vis spectrum is observed.[29] Upon the addition of acetic acid to **2**, there is no change in absorption or λ_{max}. However, upon the addition of

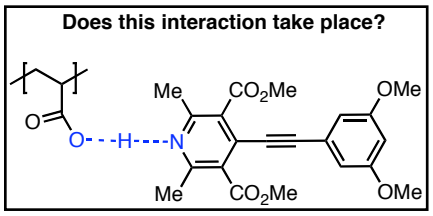

Figure 19: Hypothesized interaction between PAA and **2**.

sulfuric acid to **2**, a bathochromic shift is observed (Figure 21). At first glance, it appeared that the shift was due to protonation, but we wanted to eliminate the notion that the red shift was due to the formation of a charge transfer complex (either intermolecular or intramolecular).

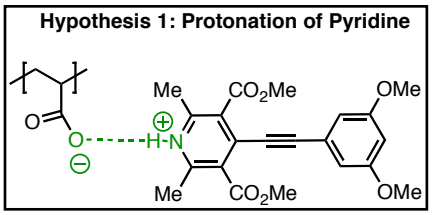

Figure 20: Hypothesis 1: protonation of **2** by PAA.

To determine whether the red shift observed upon addition of sulfuric acid was due to protonation, a series of experiments were conducted. First, we observed that upon addition of sulfuric acid to **4** (a molecule unable to form an intermolecular charge transfer complex) only an increase in absorption is observed(Figure 22, 23).[30] To determine whether an intermolecular charge transfer complex in the presence of sulfuric acid, we decided

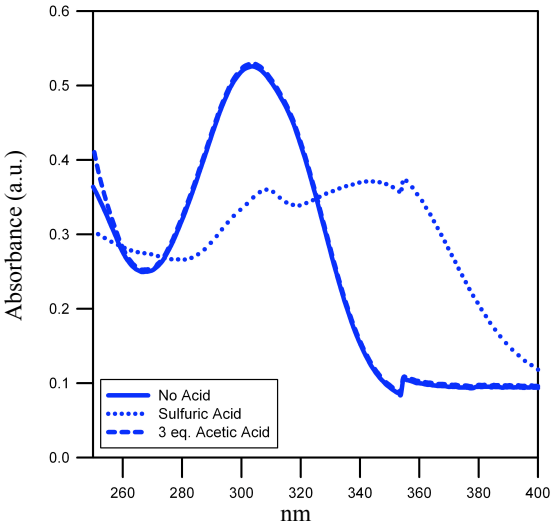

Figure 21: A bathochromic shift is observed upon the addition of sulfuric acid to **2** but not acetic acid.

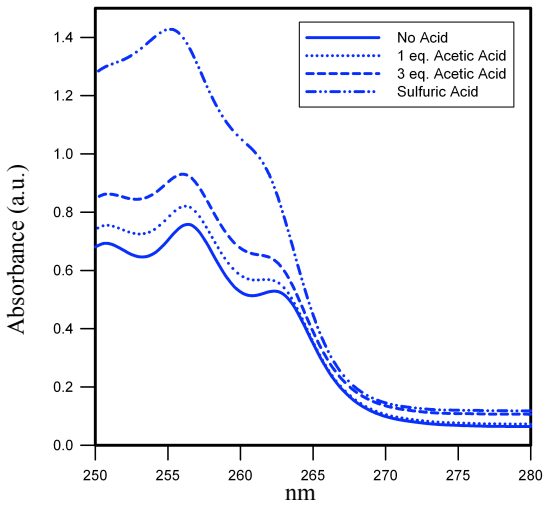

Figure 22: Upon the addition of both acetic acid and sulfuric acid to **4** an increase in absorption is observed.

to mimic the proposed charge transfer complex using another model system. To a solution of an electronically analogous electron poor pyridine **5** in the presence of sulfuric acid was titrated in a electron rich **6** (Figure 23). If an intermolecular charge transfer complex was to occur in this model system, we would expect a bathochromic shift upon the addition of **6**;

however, this was not observed (Figure 24). Overall, these model studies support the idea that, in the presence of PAA, **2** is not being fully protonated.

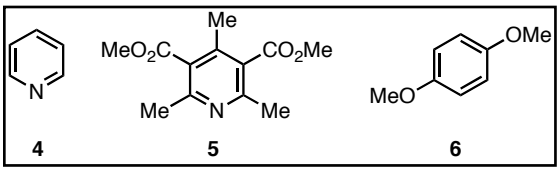

Figure 23: Compounds used in model studies.

Even though **2** is not being protonated by PAA, there is a possibility that **2** could interact with PAA via H-bonding (Figure 25). Preliminary results utilizing IR spectroscopy to probe H-bonding have not lead to any conclusions so far. The ketone of acetic acid[31] was monitored as a pyridine moiety (**4** or **5**) was titrated in. With **4**, a clear shift in the carbonyl peak suggests H-bonding between acetic acid and **4** (Figure 26). However, when the same experiment was repeated with **5**, the carbonyl peaks of **5** and acetic acid overlapped and it was unclear as to whether or not the carbonyl peak moved or not upon the addition of **5** (Figure 27). More

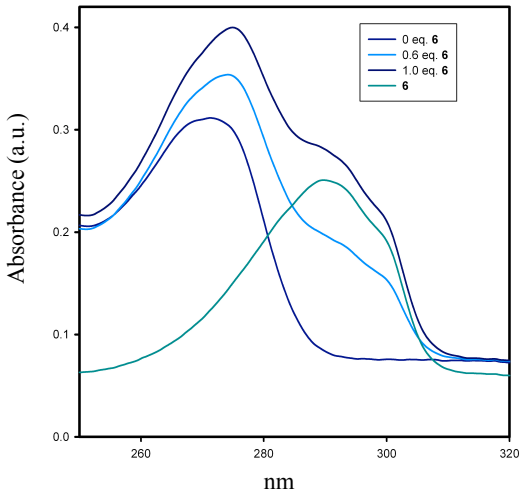

Figure 24: Upon the addition of **6** to **5**, no shift in λ_{max} of **5** is observed.

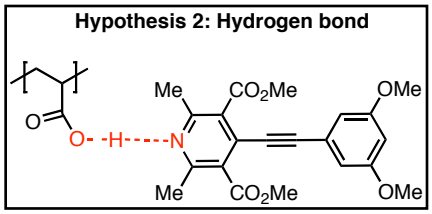

Figure 25: Hypothesis 2: Hydrogen bonding occurs between PAA and **2**.

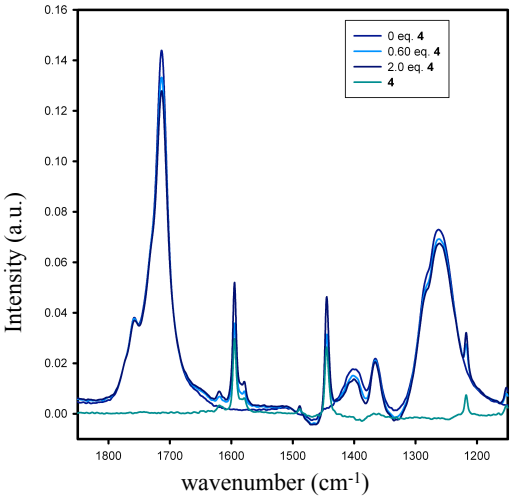

Figure 26: Addition of **4** to acetic acid.

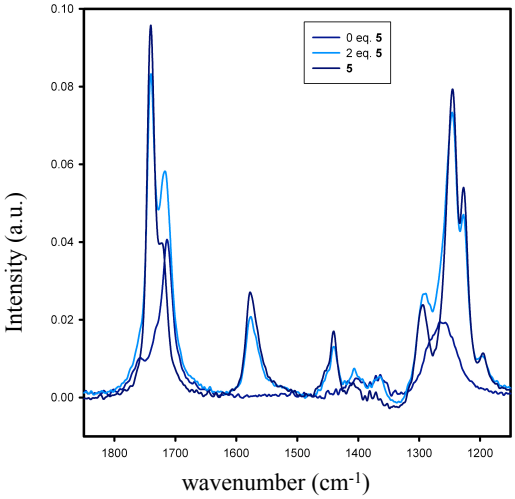

Figure 27: Addition of **5** to acetic acid.

follow-up studies need to be completed before we can determine whether or not H-bonding is occurring in this system.

FUTURE WORK

Right now, it is still unclear what interactions between the polymer and gelator lead to the decrease in the cgc of **2**. UV-Vis spectroscopy studies show that **2** is not being protonated by PAA. However, IR spectroscopy studies up to now have not conclusively shown whether or not there is H-bonding interactions between **2** and PAA; therefore, we are going to try another route to see if H-bonding interactions occur.

One way to probe intermolecular interactions of small molecules dissolved in the solution within the gel matrix is by NMR spectroscopy which has been discussed in great detail by Miravet et al.[32] They show that it is possible to monitor the interactions of small molecules with the gel network by the measurement of relaxation times, as increased relaxation times are indicative of a decreased tumbling rate of a molecule.[33] They also use 1D-NOESY spectroscopy to confirm the relaxation time information. This technique is advantageous because we can gain a deeper insight upon intermolecular interactions in the presence of the gel fiber without utilizing solid state NMR spectroscopic techniques. However, it can be difficult to interpret this data correctly, so we are also conducting variable temperature ^{1}H-NMR experiments: to a dilute solution of acetic acid, **2** will be titrated in. If H-bonding occurs, we will expect a change in the chemical shift of the proton involved in the intermolecular interaction as the temperature is varied.

Beyond elucidating the mechanism upon which PAA reduces the cgc of **2** in DMSO:H_2O systems, we want to explore many other aspects of this system. We want to determine the molecular weight dependence of PAA and gelation with **2** and explore other solvent systems and how this effects **2**'s ability to form a gel. Preliminary results by Yash Adhia suggest that there are other solvent systems that allow for a greater reduction in cgc of **2** in the presence of PAA (450 kDa).[34] Moreover, we want to continue to explore the gelation of **2** in the presence of different polymers in a myriad of solvent conditions. For all of these investigations, we want to determine how the physical properties of the gel are effected via rheology. Finally, we want to expand this method of signal amplification to other analyte-triggered gelation systems.

SUPPORTING INFORMATION

Contents:

Materials:
Silica gel (40-63 μm) was purchased from SiliCycle. All other reagent grade materials were purchased from Aldrich, Alfa Aesar, Acros, or Fisher and used without further purification unless noted.

General Experimental:
General Procedure for Heat/Cool-induced Gelation: A 4 mL vial was charged with **2**, polymer, and an organic solvent/H_2O mixture. The mixture was heated to 80 °C to form a homogenous solution and allowed to cool to 25 °C to form a gel.

NMR Spectroscopy: ^{1}H NMR spectra for all compounds were acquired in $CDCl_3$ on a Varian MR400 Spectrometer operating at 400 MHz. The chemical shift data are reported in units of δ (ppm) relative to tetramethylsilane (TMS) and referenced with residual $CHCl_3$.

Powder X-ray Diffraction: Powder X-ray diffraction (PXRD) patterns were collected at ambient temperature using a Rigaku R-AXIS SPIDER diffractometer with an imaging plate detector using graphite monochromated Cu-Kα radiation (1.5406 Å). For collections at room temperature, samples were mounted on a cryoloop. To obtain powder patterns with minimized preferred orientation, images were collected for 5 minutes while rotating the sample about the φ-axis at 10°·s-1 while oscillating ω between 120° and 180° at 1°·s-1 with χ set at 45°. Images were integrated from 2.5° to 50° 2θ with a 0.02° step size with the AreaMax[35] software package. Powder patterns were processed in Jade Plus[36] to calculate peak positions and intensities. Temperature was controlled with an Oxford Cryostream Plus.

Raman Spectroscopy: Raman spectra were obtained using a Renishaw inVia Raman Microscope equipped with a Leica microscope, RenCam CCD detector, 633 nm He-Ne laster, 1200 lines/mm grating, and 50 μm slit. Spectra were collected in extended scan mode in the range of 3600-100 cm^{-1} and analyzed using the WiRE 2.0 software package. Calibration was performed using a silicon standard.

UV-Visible Spectroscopy: UV-Vis spectra were taken on a Perkin-Elmer Lamda 850 UV-visible Spectrophotometer.

IR Absorption Spectroscopy: IR spectra were taken on a Mettler Toledo ReactIR ic10 Spectrophotometer, with AgX fiber and Silicon probe.

pH Meter: pH measurements were taken on a Beckman ϕ 300 series pH/Temperature/mV/ISE Meter.

Gas Chromatograph: GC chromatographs were taken on a Shimadzu GC 2010 with a SHRX5 column (15 m long, 0.25 mm ID, 0.25 μm film thickness). All compounds were run on the Medium-High method (1 μL injection volume, 285 °C injection temperature, 100 °C column, 0.96 mL/min column flow rate).

Synthetic Procedures

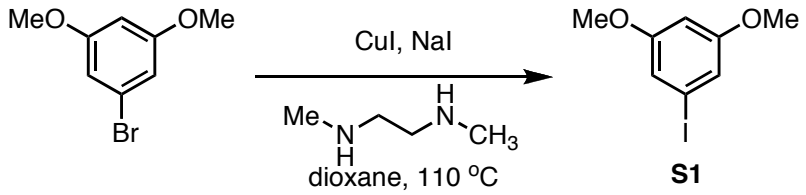

A 100 mL round-bottom flask and stir bar were oven dried and cooled to room temperature under N_2. To this was added 50 mL dioxane and the solution was degassed for 15 minutes before adding the aryl bromide (10.000 g, 0.0461 mol), NaI (13.719 g, 0.0921 mol), CuI (0.439 g, 0.00231 mol), and ligand (0.407 g, 0.00462 mol). The flask was purged with N_2 and then reflux condenser was affixed. The flask was placed in a 110 °C oil bath and stirred at high speed for 48 hours. GC of the reaction mixture confirmed the quantitative conversion to **S1**. The reaction was cooled to room temperature, quenched with aqueous ammonium hydroxide, extracted with dicholoromethane, and washed with water and brine. The organic layer was concentrated in vacuo giving a yellow oil. The oil was run through a silica plug eluted with 1:1 hexanes:ethyl acetate.[37] Concentrated under vacuo to yield white crystalline solid (73% yield). GC r_t: 5.636 minutes.

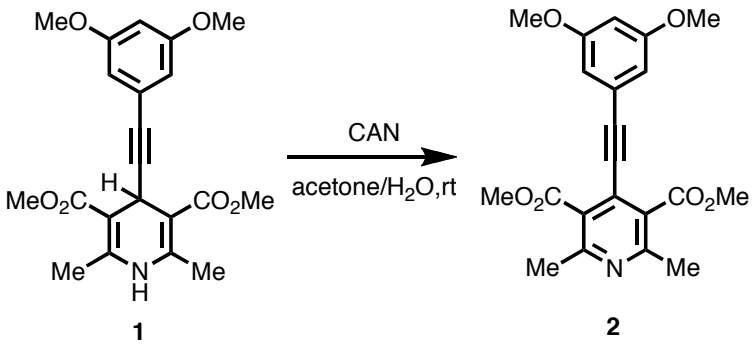

1 was obtained from A-AJM-132. A 50 mL round-bottom flask was equipped with a stir bar. To a 0.1 M solution of **1** in acetone was added dropwise a 1 M solution of ceric ammonium nitrate (CAN) in DI H_2O and stirred vigorously. After a few minutes, the solution became homogenous. DI water was added until a white precipitate formed. The precipitate was extracted with CH_2Cl_2, washed with H_2O and saturated aq. NaCl, dried with $MgSO_4$, filtered, and concentrated under vacuo. The yellow crystals were re-crystalized from hot ^{i}PrOH to give pure **2**.

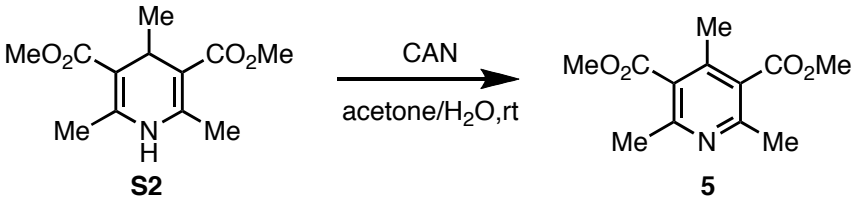

S2 was obtained from A-AJM-19. Same procedure as used for the synthesis of **2**.

^{1}H NMR Spectra

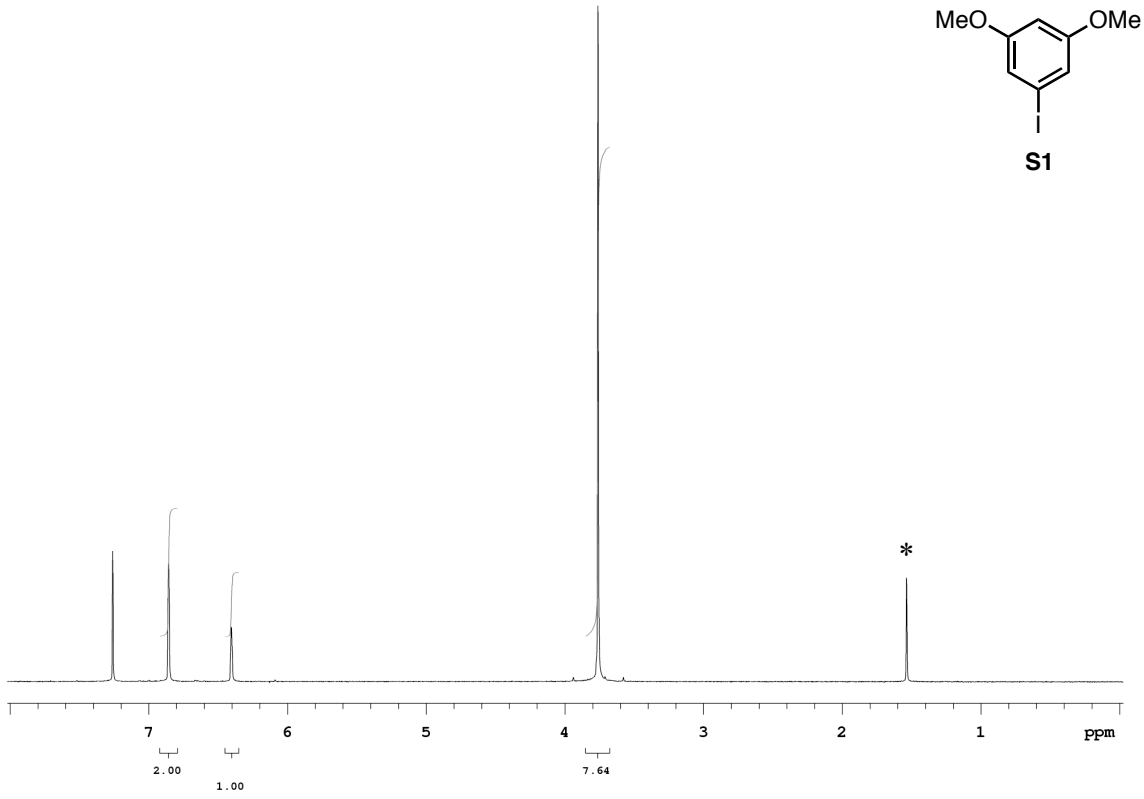

Figure S1. ^{1}H NMR spectrum of **S1**. (400 MHz, $CDCl_3$) δ 6.82 (d, 2H), 6.40 (dd, 1H), 3.76 (s, 6H). δ 6.60, 6.38 are from residual Ar-Br. *denotes H_2O peak

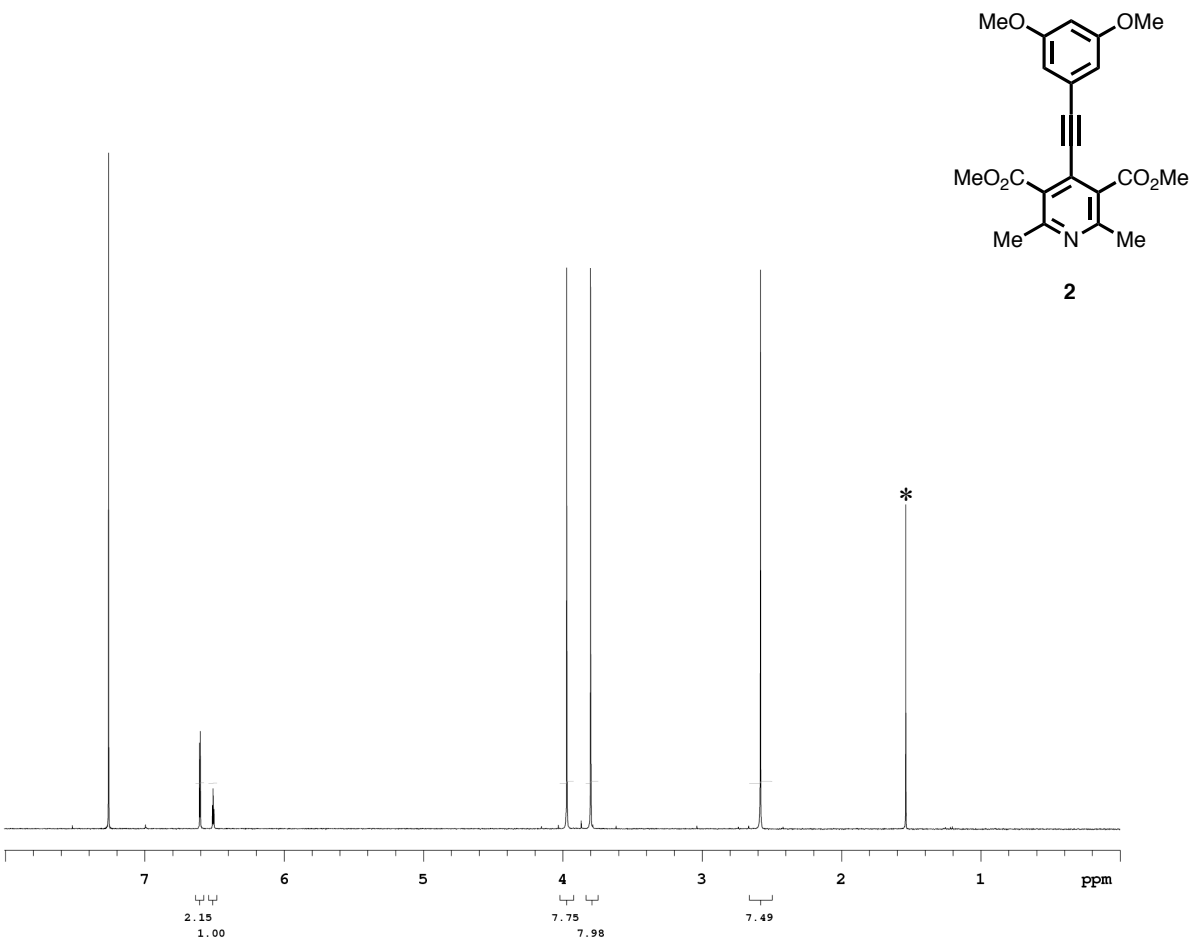

Figure S2. ^{1}H NMR spectrum of **2**. (400 MHz, $CDCl_3$) δ 6.61 (s, 2H), 6.51 (s, 1H), 3.97 (s, 6H), 3.8 (s, 6H), 2.58 (s, 6H). * denotes H_2O peak

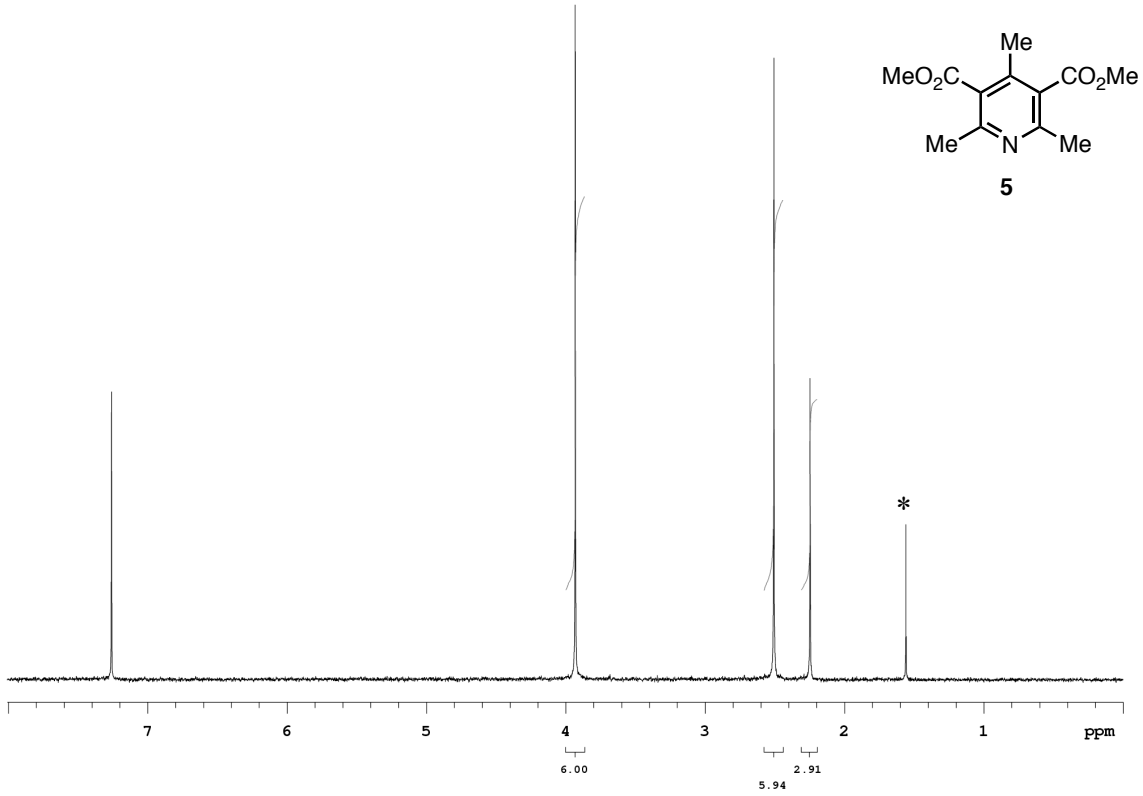

Figure S3. ^{1}H NMR spectrum of **5**. (400 MHz, $CDCl_3$) δ 3.93 (s, 6H), 2.51 (s, 6H), 2.25 (s, 3H).
***** denotes H_2O peak

Gelation Tests

To determine the cgc, 4:1 DMSO:H_2O (from a stock solution) was added in increments of 0.10 mL, heated to 80 ^oC, then allowed to cool to room temperature. If a material could self-support itself at room temperature upon inversion in a 4 mL vial, it was deemed a stable gel. This process was repeated until an unstable gel was obtained.

Experiment	[2] (mg)	[1] (mg)	CAN (mg)	Result
1	6	--	--	unstable gel
2	10	--	--	stable gel
3	3	7	--	precipitate
4	3	7	0.039	precipitate
5	6	14	--	precipitate
6	6	14	39	stable gel
7	6	4	--	unstable gel
8	7	3	--	unstable gel
9	8	2	--	unstable gel
10	9	1	--	unstable gel
11	6	4	0.011	stable gel
12	7	3	0.009	stable gel
13	8	2	0.006	unstable gel
14	9	1	0.003	stable gel

Table S1: Testing a potential alternate route to reduce the cgc of **2**.

We predicted that a mixture of **1** and **2** ([**1**] < cgc, [**2**] < cgc), in the presence of an oxidant, would allow for the formation of a stable gel in the presence of analyte in smaller quantities than previously necessary. However, this did not proceed as expected, as it was difficult to make a homogenous solution of **1**/**2**. More importantly, we were not able to consistently obtain stable gels from the oxidized **1**/**2** mixture. Sometimes we obtained a stable gel, and other times only precipitate formed upon heating and cooling

REFERENCES

[1] (a) El-Sherif, M.; Bansal, L.; Yuan, J. "Fiber Optic Sensors for Detection of Toxic and Biological Threats." *Sensors* **2007**, *7*, 3100-3118. (b) Gupta, R.; Kumar, A. "Bioactive Materials for Biomedical Applications Using Sol-Gel Technology." *Biomed. Mater.* **2008**, *3*, 1-15. (c) Calvert, P. "Hydrogels for Soft Machines." *Adv. Mater.* **2009**, *21*, 743-756.

[2] Lim, K.G.; Mottram, C. "The Use of Fraction of Exhaled Nitric Oxide in Pulmonary Practice." *Chest* **2008**, *133*, 1232-1242.

[3] Taha, Z. H. " Nitric Oxide Measurements in Biological Samples." *Talanta* **2003**, *61,* 3-10.

[4] Estroff, L. A.; Hamilton, A.D. "Water Gelation by Small Organic Molecules." *Chem. Rev.* **2004**, *104,* 1201-1217.

[5] Chen, J.; McNeil, A. J. "Analyte-Triggered Gelation: Initiating Self-Assembly via Oxidation-Induced Planarization." *J. Am. Chem. Soc.* **2008**, *130*, 16496-16497.

[6] Yang, Z.; Ho, P.-L.; Liang, G.; Xu, B. "Using β-Lactamase to Trigger Supramolecular Hydrogelation." *J. Am. Chem. Soc.* **2007**, *129,* 266-267.

[7] Tysseling-Mattiace, V. M.; Sahni, V.; Niece, K. L.; Birch, D.; Czeisler, C.; Fehlings, M. G.; Stupp, S. I.; Kessler, J. A. "Self-assembling Nanofibers Inhibit Glial Scar Formation and Promote Elongation After Spinal Cord Injury." *J. Neurosci.* **2008**, *28*, 3814-3823.

[8] Hirst, A.; Smith, D. K. "High-Tech Applications of Self-Assembling Supramolecular Nanostructured Gel-Phase Materials: From Regenerative Medicine to Electronic Devices." *Angew. Chem. Int. Ed.* **2008**, *47,* 8002-8018.

[9] (a) Hirst, A. R.; Coates, I. A.; Boucheteau, T. R.; Miravet, J. F.; Escuder, B.; Castelletto, V.; Hamley, I. W.; Smith, D. K. "Low-molecular-weight Gelators: Elucidating the Principles of Gelation Based on Gelator Solubility and a Cooperative Self-Assembly Model." *J. Am. Chem. Soc.* **2008***, 130,* 9113-9121. (b) Jonkheijm, P.; Van der schoot, P.; Schenning, A. P. H. J.; Meijer, E. W. "Probing the Solvent-Assisted Nucleation Pathway in Chemical Self-Assembly." *Science* **2006**, *313,* 80-83. (c) Tan, G.; John, V. T.; McPherson, G. L. "Nucleation and Growth Characteristics of a Binary Low-Mass Organogel." *Langmuir* **2006**, *22,* 7416-7420.

[10] Zhang, T. H.; Liu, X. Y. "Nucleation: What Happens at the Initial Stage?" *Angew. Chem. Int. Ed.* **2009**, *48,* 1308-1312.

[11] Liu, X. Y.; Sawant, P. D.; Tan, W. B.; Noor, I. B. M.; Prasmesti, C.; Chen, B. H. "Creating New Supramolecular Materials by Architecture of Three-Dimensional Nanocrystal Fiber Networks." *J. Am. Chem. Soc.* **2002**, *124,* 15055-15063.

[12] Singh, S. "Sensors- An Effective Approach of the Detection of Explosives." *J. Haz. Mater.* **2007**, *144,* 15-28.

[13] Thomas, S. W.; Joly, G. D.; Swager, T. M. "Chemical Sensors Based on Amplifying Fluorescent Conjugated Polymers." *Chem. Rev.* **2007**, *107,* 1339-1386.

[14] Heller, D. A.; Jin, H.; Martinez, B. M.; Patel, D.; Miller, B. M.; Yeung, T.; Jena, P. V.; Hobartner, C.; Ha, T.; Silverman, S. K.; Strano, M. S. "Multimodal Optical Sensing and Analyte Specificity Using Single-Walled Carbon Nanotubes." *Nature Nanotechnology* **2008**, *4,* 114-120.

[15] For a recent example, see: Shome, A.; Debnath, S.; Das, P. K. "Head Group Modulated pH-Responsive Hydrogel of Amino Acid-Based Amphiphiles: Entrapment and Release of Cytochrome *c* and Vitamin B_{12}." *Langmuir* **2008**, *24*, 4280-4288.

[16] For a recent example, see: Matsumoto, S.; Yamaguchi, S.; Ueno, S.; Komatsu, H.; Ikeda, M.; Ishizuka, K.; Iko, Y.; Tabata, K. V.; Aoki, H.; Ito, S.; Noji, H.; Hamachi, I. "Photo Gel-Sol/Sol-Gel Transition and Its Patterning of a Supramolecular Hydrogel as Stimuli-Responsive Biomaterials." *Chem. Eur. J.* **2008**, *14*, 3977-3986.

[17] Hirst, A. R.; Smith, D. K. "Two-Component Gel-Phase Materials- Highly Tunable Self-Assembling Systems." *Chem. Eur. J.* **2005**, *11,* 5496-5508.

[18] Liu, Q.; Wang, Y.; Li, W.; Wu, L. "Structural Characterization and Chemical Response of Ag-coordinated Supramolecular Gel." *Langmuir* **2007**, *23,* 8217-8223.

[19] Escuder, B.; Miravet, J. F.; Saez, J. A. "Molecular Recognition Through Divalent Interactions with a Self-assembled Fibrillar Network of a Supramolecular Organogel." *Org. Biomol. Chem.* **2008**, *6,* 4378-4383.

[20] Hirst, A. R.; Miravet, J. F.; Escuder, B.; Noirez, L.; Castelletto, V.; Hamley, I.W.; Smith, D.K. "Self-Assembly of Two-Component Gels: Stoichiometric Control and Component Selection." *Chem. Eur. J.* **2009**, *15,* 372-379.

[21] Lent, T. H.; McNeil, A. J. "Gelation of Low Molecular Weight Molecules with Polymers for Signal Amplification in Sensing." Poster presentation given at the 237th National Meeting of the American Chemical Society, March 22-26, 2009, Salt Lake City, Utah.

[22] (a) de Loos, M.; van Esch, J.; Kellogg, R. M.; Feringa, B. L. "Chiral Recognition in bis-urea-based Aggregates and Organogels Through Cooperative Interactions." *Angew. Chem. Int. Ed.* **2001**, *40,* 613-616. (b) Rodrigues-Llansola, F.; Miravet, J. F., Escuder, B. "Supramolecular Gel Formation and Self-Correction Induced by Aggregation-Driven Conformational Changes." *Chem. Commun.* **2009**, 209-211. (c) Brand, T.; Nolis, P.; Richter, S.; Berger, S. "NMR Study of the Gelation of a Designed Gelator." *Magn. Reson. Chem.* **2008,** *46,* 545-549. (d) Rizkov, D.; Mizrahi, S.; Gun, J.; Hoffman, R.; Melman, A.; Lev, O. "Nonstoichiometric Gelation of Cyclodextrins and Induced Planar Guests." *Langmuir* **2008**, *24,* 11902-11910. (e) de Greef, T. F. A.; Nieuwenhuizen, M. M. L.; Stals, P. J. M.; Fitie, C.F.C.; Palmans, A. R. A.; Sijbesma, R. P.; Meijer, E.W. "The Influence of Ethylene Glycol Chains on the Thermodynamics of Hydrogen-Bonded Supramolecular Assemblies in Apolar Solvents." *Chem. Commun.* **2008**, 4306-4308.

[23] (a) Becerril, J.; Burguete, M. I.; Escuder, B.; Galindo, F.; Gavara, R.; Miravet, J. F.; Luis, S. V.; Peris, G. "Self-Assembly of Small Peptidomimetic Cyclophanes." *Chem. Eur. J.* **2004**, *10,* 3879-3890. (b) Escuder, B.; Marti, S.; Miravet, J. F. "Organogel Formation by Coaggregation of Adaptable Amido-carbamates and their Tetra-amide Analogues." *Langmuir* **2005**, *21*, 6776-6787.

[24] Wackerly, J. M.; Moore, J. S. "Cooperative Self-Assembly of Oligo(*m*-phenyleneethynylenes) into Supramolecular Coordination Polymers." *Macromolecules* **2006**, *39,* 7269-7276.

[25] Li, J. L.; Liu, X. Y.; Strom, C. S.; Xiong, J. Y. "Engineering of Small Molecule Organogels by Design of the Nanometer Structure of Fiber Networks." *Adv. Mater.* **2006**, *18,* 2574-2578.

[26] J. Brandup and E. H. Immergut, Eds., *Polymer Handbook*, 4th Ed., Wiley Interscience, New York, 2005; Schuld, N.; Wolf, B. A., pp. VII/250.

[27] (a) Zhao, J.; Larock, R. C. "Synthesis of Substituted Carbazoles, Indoles, and Dibenzofurans by Vinylic to Aryl Palladium Migration." *J. Org. Chem.* **2006**, *71*, 5340-5348. (b) Wendt, M. D.; Rockway, T. W.; Geyer, A.; McClellan, W.; Weitzberg, M.; Zhao, X.; Mantei, R.; Nienaber, V. L.; Stewart, K.; Klinghofer, V.; Giranda, V. L. "Identification of Novel Binding Interactions in the Development of Potent, Selective 2-Naphthamidine Inhibitors of Urokinase. Synthesis, Structural Analysis, and SAR of *N*-Phenyl Amide 6-Substitution." *J. Med. Chem.* **2004**, *47*, 303-324. (c) Krasnokutskaya, E. A.; Semenischeva, N. I.; Filimonov, V. D.; Knochel, P. "A New, One-Step, Effective Protocol for the Iodination of Aromatic and Heterocyclic Compounds via Aprotic Diazotization of Amines." *Synthesis* **2007**, *1*, 81-84. (d) Ishii, M.; Matsumura, S.; Toshima, K. "Target-Selective Degradation of Oligosaccharides by a Light-Activated Small-Molecule-Lectin Hybrid." *Angew. Chem. Int. Ed.* **2007**, *46*, 8396-8399.

[28] Obtained by Yash Adhia and Jing Chen. Unpublished results.

[29] Duggeli, M.; Christen, T.; von Zelewsky, A. "Protonation Behaviour of Chiral Tetradentate Polypyridines Dervied from α-Pinene: Chiralization of the Proton." *Chem. Eur. J.* **2005**, *11*, 185-194.

[30] *Principles of Instrumental Analysis, 6th Ed.*; Skoog, D.A.; Holler, F.J.; Crouch, S.R., Eds.; Thomson: Canada, 2007.

[31] The probe of the React-IR did not allow us to monitor the hydroxyl group of acetic acid.

[32] Escuder, B.; Llusar, M.; Miravet, J. F. "Insight on the NMR Study of Supramolecular Gels and its Application to Monitor Molecular Recognition on Self-Assembled Fibers." *J. Org. Chem.* **2006**, *71*, 7747-7752.

[33] A useful resource: *High-Resolution NMR Techniques in Organic Chemistry, 2nd Ed.*; Claridge, T., Ed.; Elsevier: Amsterdam, New York, 2009.

[34] Adhia, Y.; McNeil, A. J. Unpublished results.

[35] AreaMax 2.0.0.4 e.; Rigaku, 2005.

[36] Jade Plus 8.2 ed.; Materials Data, Inc., 1995-2007.

[37] Klapars, A.; Buchwald, S. "Copper-Catalyzed Halogen Exchange in Aryl Halides: An Aromatic Finkelstein Reaction." *J. Am. Chem. Soc.* **2002**, *124*, 14844-14845.